Nuclear Instruments and Methods in Physics Research B79 (1993) 15–20
North-Holland

NIM B
Beam Interactions with Materials & Atoms

Ion-induced electron emission in grazing ion–surface collisions

F.J. García de Abajo

Dpto. de Ciencias de la Computación e Inteligencia Artificial, Facultad de Informática, Universidad del País Vasco, Aptdo. 649, 20080 San Sebastián, Spain

P.M. Echenique

Dpto. de Física de Materiales, Facultad de Química, Universidad del País Vasco, Aptdo. 1072, 20080 San Sebastián, Spain

The distribution of low-energy electrons emitted from a solid when a swift ion interacts with its surface under grazing incidence conditions is obtained using first-order time-dependent perturbation theory. The response of the surface is calculated from the specular-reflection model and the random-phase approximation for the dielectric function of the bulk material. The electrons are described in terms of independent states, that are solutions of the Schrödinger equation with a finite square barrier potential. A broad peak in energy, corresponding to the excitation of surface plasmons, is predicted to appear in the energy spectrum. The angular dependence of the emission is also analyzed. The electrons are found to be preferentially emitted in the normal and forward directions.

The electron emission from solids due to ion bombardment has been the subject of much research over the past several decades [1–3]. The process has been usually analyzed by studying separately the excitation and transport mechanisms [3], the excitation being calculated from the bulk properties of the material. Nevertheless, the presence of the surface may play an important role in low-energy electron emission, where the mean free path of the emitted electrons is of the same order as the characteristic length of screening of the surface potential ($\approx v/\omega_s$, where v is the ion velocity and ω_s is the classical surface plasma frequency). This is especially true in the case under consideration, where the ion travels parallel with the surface and outside the solid.

Here we provide a theory of direct low-energy ion-induced electron emission under grazing incidence conditions. We combine a reasonable description of the interaction potential and electron wave functions that take the presence of the surface into account. This may be seen as a first step toward the understanding of recent experimental results on the detection of secondary electrons in coincidence with energy-loss events of the primary beam [4]. The latter seem to give information on the mechanisms of electron excitation from solids and on the role played by bulk and surface plasmons [5].

Atomic units will be used throughout this paper unless otherwise specified. The position vector will be $\boldsymbol{r} = (\boldsymbol{R}, z)$. Upper case vectors will stand for components parallel to the surface, chosen to lie in the plane $z = 0$.

The conduction band of the solid is described in terms of the Sommerfeld model of a metal, in which independent electrons are confined in the $z < 0$ region by a square barrier $V = V_0\theta(z)$, where $V_0 = E_F + \Phi$, E_F is the Fermi energy and Φ is the work function. The probability that an electron of the conduction band is ejected to a free state is calculated using first-order time-dependent perturbation theory. The electron states, represented by solutions of the Schrödinger equation with the above potential, can be written as

$$\psi_l^\sigma(\boldsymbol{r}) = \frac{e^{i\boldsymbol{Q}\cdot\boldsymbol{R}}}{\sqrt{A}}\varphi_{l_z}^\sigma(z), \tag{1}$$

where A is the area of the surface and $\boldsymbol{l} = (\boldsymbol{Q}, l_z)$ is the momentum of the electron in the solid side. The

energy of the state with respect to the bottom of the conduction band is given by $l^2/2$. σ indicates the character of the state. Using δ-function normalization in the z-direction one gets:
i) $\sigma = 0$. Bound states ($l_z^2 \le 2V_0$):

$$\varphi_{l_z}^0(z) = \frac{1}{\sqrt{2\pi}}\left\{\left[\frac{l_z - ip}{l_z + ip}e^{-il_z z} + e^{il_z z}\right]\theta(-z) + \frac{2l_z}{l_z + ip}e^{-pz}\theta(z)\right\}, \tag{2a}$$

where $p = (2V_0 - l_z^2)^{1/2}$.
ii) $\sigma = \pm$. Free states, classified in two families of orthogonal states that, together with eq. (2a), form a complete system. Namely,
iia) $\sigma = +$, outgoing states (OUT):

$$\varphi_{l_z}^+(z) = \frac{1}{\sqrt{2\pi}}\left\{\left[\frac{l_z - k_z}{l_z + k_z}e^{-il_z z} + e^{il_z z}\right]\theta(-z) + \frac{2l_z}{l_z + k_z}e^{ik_z z}\theta(z)\right\}, \tag{2b}$$

iib) $\sigma = -$, incoming states (IN):

$$\varphi_{l_z}^-(z) = \sqrt{\frac{l_z/k_z}{2\pi}}\left\{\frac{2k_z}{k_z + l_z}e^{-il_z z}\theta(-z) + \left[\frac{k_z - l_z}{k_z + l_z}e^{ik_z z} + e^{-ik_z z}\right]\theta(z)\right\}, \tag{2c}$$

where $k_z = (l_z^2 - 2V_0)^{1/2}$ is the normal component of the electron momentum in the vacuum.

Transport of the emitted electrons up to the surface is accounted for through an exponential factor e^{qz} multiplying each final electron state in the solid side, where $q = l/(2\lambda l_z)$ and λ is the electron mean free path.

The screened potential induced by interaction of the ion with the solid is described in Fourier transform space in time and in the coordinates parallel to the surface:

$$\phi(r, t) = \frac{1}{(2\pi)^3}\int dQ \int_{-\infty}^{\infty} d\omega\, e^{i(Q\cdot R - \omega t)}\phi(Q, z, \omega). \tag{3}$$

The perturbed part of the wave function of a given initial state in the Fermi sea caused by transitions to free states can be expressed in terms of the potential of eq. (3):

$$\Delta\psi(r, t) = \frac{1}{(2\pi)^3}\int d\omega \int dQ_l \frac{e^{iQ_l\cdot R}}{\sqrt{A}}\, e^{-i(\epsilon_0 + \omega)t} \sum_{\sigma = \pm}\int_0^{\infty} dl_z \varphi_{l_z}^{\sigma}(z)$$
$$\times \frac{e^{-i(\epsilon_1 - \epsilon_0 - \omega)(t - t_0)} - 1}{\epsilon_1 - \epsilon_0 - \omega}\langle \varphi_{l_z}^{\sigma} | \phi(Q_1 - Q_0, z, \omega) | \varphi_{l_z^0}^0\rangle, \tag{4}$$

where $l_0 = (Q_0, l_z^0)$ and $l_1 = (Q_1, l_z)$ are the initial and final momenta of the electron, $\epsilon_0 = l_0^2/2 < E_F$ and $\epsilon_1 = l_1^2/2 > V_0$ are the initial and final energies, respectively, and t_0 is the time when the interaction is switched on.

The connection of this theory with measurement can be achieved by analyzing the asymptotic behavior of eq. (4). Following the method first used by Bethe [6], particularized to the case of electron emission from surfaces by Wilems [7], one finds

$$\Delta\psi(r, t) \approx \int dk \frac{e^{ik\cdot r}}{\sqrt{2\pi A}} e^{-ie_1 t}\theta[k_z(t - t_0) - z] M_{k \leftarrow l_0} \qquad (z \to \infty), \tag{5}$$

where

$$M_{k \leftarrow l_0} = \frac{-i}{2\pi}\left(\frac{k_z}{k_z + l_z}\right)\left[2\langle \varphi_{l_z}^+ | \phi(Q, z, \omega) | \varphi_{l_z^0}^0\rangle + \frac{k_z - l_z}{\sqrt{k_z l_z}}\langle \varphi_{l_z}^- | \phi(Q, z, \omega) | \varphi_{l_z^0}^0\rangle\right]. \tag{6}$$

Here $\boldsymbol{k} = (\boldsymbol{Q}_\parallel, k_z)$ is the momentum of the electron in the vacuum, and $\boldsymbol{Q} = \boldsymbol{Q}_\parallel - \boldsymbol{Q}_0$. Eq. (5) expresses the fact that the final state is asymptotically a combination of plane waves. For z larger than $k_z(t - t_0)$, the $\boldsymbol{k}$-component of the perturbed wave function vanishes: when the electron is emitted with momentum $\boldsymbol{k}$, it takes a time not smaller than z/k_z to arrive at z. In the limit $t_0 \to -\infty$, the step function in eq. (5) is 1.

Assume that the ion follows an external parallel trajectory. $\phi(\boldsymbol{Q}, z, \omega)$ is obtained making use of the specular-reflection model, introduced by Ritchie and Marusak [8] in the study of the surface plasmon dispersion relation and independently discussed by Wagner [9]. In this model the surface response function is expressed in terms of the dielectric function of the bulk material $\epsilon(k, \omega)$. It is equivalent to the semiclassical infinite barrier model [10,11]. Calculations of the surface potential and the energy loss of particles traveling in the vicinity of flat surfaces have already been carried out using this model [12–14]. We find the following result [14]:

$$\phi(\boldsymbol{Q}, z, \omega) = \frac{(2\pi)^2 Z_1 \delta(\omega - \boldsymbol{Q}\cdot\boldsymbol{V})}{Q} \left\{ \left[\frac{2\mathrm{e}^{-Qz_0}}{\epsilon_s(\boldsymbol{Q}, \omega) + 1} \epsilon_s(\boldsymbol{Q}, z, \omega) \right] \theta(-z) + \left[\frac{\epsilon_s(\boldsymbol{Q}, \omega) - 1}{\epsilon_s(\boldsymbol{Q}, \omega) + 1} \mathrm{e}^{-Q(z+z_0)} + \mathrm{e}^{-Q|z-z_0|} \right] \theta(z) \right\}, \tag{7}$$

where z_0 is the distance from the ion to the surface, Z_1 and $\boldsymbol{V}$ denote the charge and velocity of the ion,

$$\epsilon_s(\boldsymbol{Q}, z, \omega) = \frac{Q}{\pi} \int \frac{\mathrm{d}k_z}{k^2} \frac{\mathrm{e}^{\mathrm{i}k_z z}}{\epsilon(k, \omega)},$$

$k^2 = Q^2 + k_z^2$, and $\epsilon_s(\boldsymbol{Q}, \omega) = \epsilon_s(\boldsymbol{Q}, 0, \omega)$ is the surface dielectric function [15]. The last term in eq. (7) for $z > 0$ represents the direct Coulomb potential. Inserting eqs. (2) and (7) into eq. (6) one obtains

$$M_{\boldsymbol{k} \leftarrow \boldsymbol{l}_0} = m_{\boldsymbol{k} \leftarrow \boldsymbol{l}_0} \delta(\omega - \boldsymbol{Q}\cdot\boldsymbol{V}),$$

where

$$m_{\boldsymbol{k} \leftarrow \boldsymbol{l}_0} = \frac{-\mathrm{i}Z_1}{\pi Q} \left\{ \frac{l_z^0}{l_z^0 + \mathrm{i}p} \left[I^+(p + \mathrm{i}k_z) + \frac{k_z - l_z}{k_z + l_z} I^+(p - \mathrm{i}k_z) \right] + \frac{k_z}{k_z + l_z} \left[I^-\big(q - \mathrm{i}(l_z - l_z^0)\big) + \frac{l_z^0 - \mathrm{i}p}{l_z^0 + \mathrm{i}p} I^-\big(q - \mathrm{i}(l_z + l_z^0)\big) \right] \right\},$$

$$I^+(a) = \left\{ \frac{1}{Q + a} \left[\frac{\epsilon_s(\boldsymbol{Q}, \omega) - 1}{\epsilon_s(\boldsymbol{Q}, \omega) + 1} \right] - \frac{1}{Q - a} \right\} \mathrm{e}^{-Qz_0} + \frac{2Q\,\mathrm{e}^{-az_0}}{Q^2 - a^2},$$

$$I^-(a) = \frac{2a\,\mathrm{e}^{-Qz_0}}{(Q^2 - a^2)[\epsilon_s(\boldsymbol{Q}, \omega) + 1]} \left\{ \frac{2Q}{\pi} \int_0^\infty \frac{\mathrm{d}k_z}{(k_z^2 + a^2)} \frac{1}{\epsilon(k, \omega)} - \epsilon_s(\boldsymbol{Q}, \omega) \right\},$$

and $q = l/(2\lambda l_z)$ is the coefficient of the exponential attenuation of the final states for $z < 0$. This coefficient accounts phenomenologically for the finite mean free path λ of these electrons.

The differential rate at which electrons escape from the surface is obtained by calculating the flux through a plane parallel to the surface and located at a large distance from the solid. Using eq. (5) to calculate the current density, inserting the result into the continuity equation, and finally integrating over all the initial states in the Fermi sea, one finds:

$$\frac{\mathrm{d}W}{\mathrm{d}\boldsymbol{k}} = \frac{1}{\pi} \int \mathrm{d}\boldsymbol{Q}_0\, \theta(E_\mathrm{F} - \epsilon_0) \theta\big(l^2 - Q_0^2 - 2\boldsymbol{Q}\cdot\boldsymbol{V}\big) \frac{1}{l_z^0} |m_{\boldsymbol{k} \leftarrow \boldsymbol{l}_0}|^2, \tag{8}$$

with $(l_z^0)^2 = l^2 - Q_0^2 - 2\boldsymbol{Q}\cdot\boldsymbol{V}$ and $\omega = \boldsymbol{Q}\cdot\boldsymbol{V}$. The step functions in eq. (8) restrict the integration domain to that shown in fig. 1. Looking at the figure one sees that the emission can only be observed when the

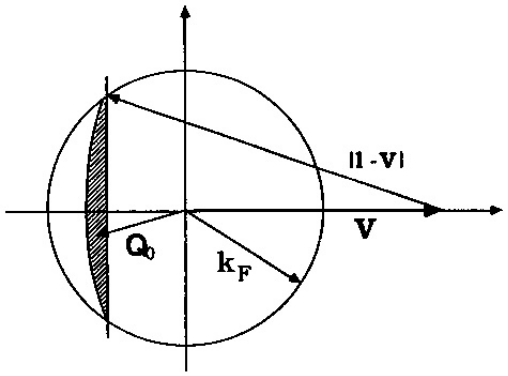

Fig. 1. The domain of integration in eq. (8) is represented here by the shadowed region in the Q_0-plane. k_F is the Fermi momentum, l is the momentum of the emitted electron in the solid side and v is the velocity of the ion.

condition $|v - v_F| \leq |l - v| \leq v + v_F$ is fulfilled. This condition is the same as the one obtained for electron excitation in the bulk material [2].

The matrix element $M_{k \leftarrow i_0}$ is made up of two terms coming from IN and OUT states, respectively. Consequently, its square contains an interference term between these states.

The energy dependence of the rate of emission in the direction normal to the surface (i.e., dW/dk with $Q_1 = 0$, eq. (8)) is shown in fig. 2 for the case of a proton traveling parallel to an aluminum surface and for $z_0 = 0$, 2, and 5. The RPA bulk dielectric function has been used here [16]. The emission decreases markedly for energies above 10–12 eV in all cases. Most of the low-energy emission is concentrated in the region 2–10 eV. Electrons close to the Fermi level, where the density of states has its maximum value, that are excited by surface plasmons give the main contribution to the broad peak observed in the figure. Further, when z_0 increases, the larger contribution to the integral (8) arises from states that make $Q = |Q_1 - Q_0|$ as small as possible, due to the exponential decay with Qz_0 observed in the induced part of the potential (see eq. (7)). In the case of normal emission, where $l = l_z$, conservation of parallel momentum leads to $Q = Q_0$, so that making Q small means lowering $|l - v|$ according to fig. 1, that is, lowering l. This results in a shift of the emission towards lower energies with increasing ion–surface separation z_0, as shown in the figure for $z_0 = 5$ a.u. The maximum is near the value

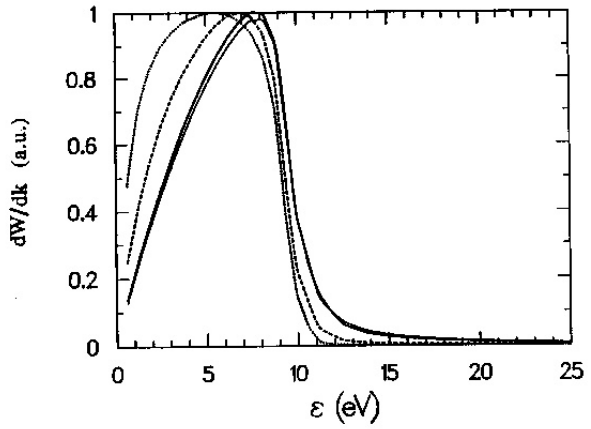

Fig. 2. Energy dependence of the rate of electron emission in the direction normal to an aluminum surface ($r_s = 2.07$ and damping $\gamma = 0.5$ eV) induced by proton bombardment under grazing incidence conditions, according to eq. (8), for various separations of the ion with respect to the surface: $z_0 = 0$ (continuous curves), $z_0 = 2$ a.u. (dashed curve), and $z_0 = 5$ a.u. (dotted curve). Continuous, dashed and dotted curves are multiplied by a factor of 5.56, 13.4 and 51.9 respectively. The ion velocity is $v = 2.5$ a.u. The ion–surface interaction has been calculated using the specular-reflection model [8] (eq. (7)) and the RPA dielectric function [16]. We have taken $q = 0.1$ a.u. (narrow continuous curve) and $q = 0.01$ a.u. (rest).

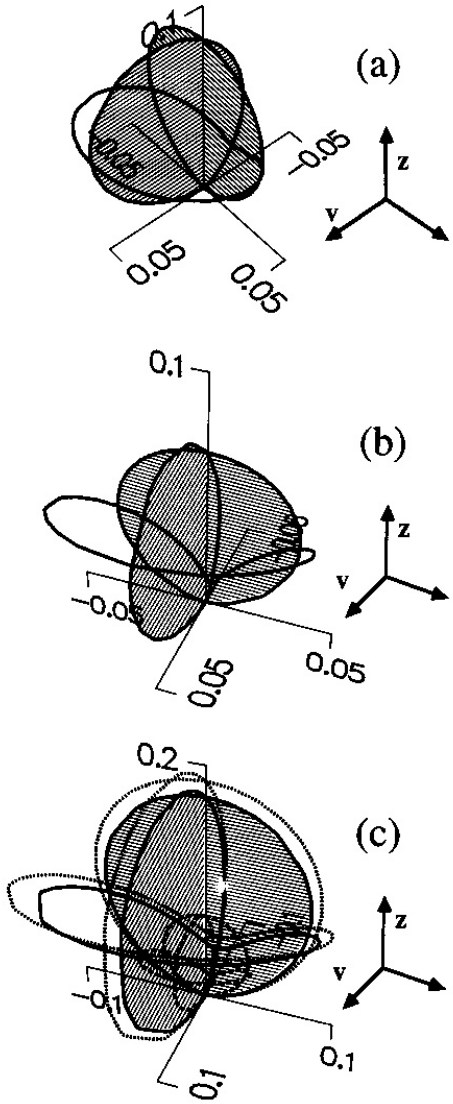

Fig. 3. Angular dependence of the electron emission rate under the same conditions as in fig. 2 with $q = 0.01$ a.u. and $v = 2.5$ a.u. The distance to the origin represents the transition rate as given by eq. (8). Different energies of the emitted electrons have been considered: (a) 2.5 eV, (b) 10 eV and (c) $\omega_s - \phi = 6.9$ eV. We have taken $z_0 = 0$ (continuous curves), $z_0 = 2$ a.u. (dashed curves in (c)) and $z_0 = 5$ a.u. (dotted curves in (c), multiplied by a factor of 10). The directions of the velocity and the surface normal have been indicated in the accompanying insets.

$\omega_s - \phi \approx 6.9$ eV, but for smaller z_0 it lies at larger energies. This behavior is due to the dispersion of the surface plasmons, whose energy can range from 11.2 eV (for $Q = 0$) to ≈ 23.6 eV where the plasmon curve enters the continuum of electron–hole pair excitations. The emission probability decreases very rapidly with increasing z_0.

Spatial attenuation of the final electron states in the solid, accounted for through the factor e^{qz}, seems not to affect these results very much. The results obtained using $q = 0.1$ (narrow continuous curve for $z_0 = 0$ in fig. 2) do not differ much from those obtained with $q = 0.01$ (thick curve). The explanation may be found in the fact that the characteristic range of the screened potential when the ion is outside the medium is only $\approx v/\omega_s \approx 3.2$ Å for aluminum when $v = 2.5$ a.u. This is smaller than the typical mean free path of the emitted electrons, which is > 20 Å in the bulk for energies smaller than 10 eV [17]. The values of q considered above are obtained from mean free paths $\lambda = 2.6$ Å and $\lambda = 26$ Å in the case of normal emission.

The angular dependence of the emission rate is shown in figs. 3a–3c for different energies of the emitted electrons (see the caption). The direction of the maximum of emission forms an angle of $\approx 55–75°$ with the velocity vector and lies in the plane defined by the velocity and the surface normal.

Acknowledgements

One of the authors (F.J.G.A.) is grateful to Professor R.H. Ritchie for his many helpful suggestions. The authors gratefully acknowledge help and support by the Departamento de Educación del Gobierno Vasco, Gipuzkoako Foru Aldundia and the Spanish Comisión Asesora Científica y Técnica (CAICYT).

References

[1] R.H. Ritchie, Phys. Rev. 114 (1959) 644.
[2] D.K. Brice and P. Sigmund, K. Dan. Vidensk. Selsk. Mat. Fys. Medd. 40 (1980) no. 5.
[3] M. Rösler and W. Brauer, Phys. Status Solidi B126 (1984) 629; 148 (1988) 213.
[4] F.J. Pijper and P. Kruit, Phys. Rev. B44 (1991) 9192.
[5] M.S. Chung and T.E. Everhart, Phys. Rev. B15 (1977) 4699.
[6] H. Bethe, Ann. der Phys. 4 (1930) 443. (See also the explanation of the method given in N.F. Mott and H.S.W. Massey, The Theory of Atomic Collisions, 3rd ed. (Oxford University Press, Oxford, England, 1965).)
[7] R.E. Wilems, Ph.D. thesis, University of Tennessee, Oak Ridge National Laboratory report ORNL-TM-2101 (1968).
[8] R.H. Ritchie and A.L. Marusak, Surf. Sci. 4 (1966) 234.
[9] D. Wagner, Z. Naturforsch. A21 (1966) 634.
[10] F. García-Moliner and F. Flores, Introduction to the Theory of Solid Surfaces (Cambridge University Press, Cambridge, England, 1979).
[11] Z. Penzar and M. Sŭnjič, Phys. Scripta 30 (1984) 453.
[12] R. Núñez, P.M. Echenique and R.H. Ritchie, J. Phys. C13 (1980) 4229.
[13] P.M. Echenique, Philos. Mag. B52 (1985) L9.
[14] F.J. García de Abajo and P.M. Echenique, Phys. Rev. B46 (1992) 2663.
[15] D.M. Newns, Phys. Rev. B1 (1970) 3304.
[16] J. Lindhard, K. Dan. Vidensk. Selsk. Mat. Fys. Medd. 28 (1954) no. 8.
[17] C.J. Tung, J.C. Ashley and R.H. Ritchie, Surf. Sci. 81 (1979) 427;
D.R. Penn, Phys. Rev. B35 (1987) 482.